



Four novel mutations of *FAM20A* in amelogenesis imperfecta type IG and review of literature for its genotype and phenotype spectra

Issree Nitayavardhana¹ · Thanakorn Theerapanon^{2,3} · Chalurmpon Srichomthong^{4,5} · Sakkayaphab Piwluang⁶ · Duangdao Wichadaku^{7,8,9} · Thantrira Porntaveetus^{1,2} · Vorasuk Shotelersuk^{4,5}

Received: 14 January 2020 / Accepted: 18 March 2020
© Springer-Verlag GmbH Germany, part of Springer Nature 2020

Abstract

Amelogenesis imperfecta type IG (AIIG) is caused by mutations in *FAM20A*. Genotypic and phenotypic features of AIIG are diverse and their full spectra remain to be characterized. The aim of this study was to identify and summarize variants in *FAM20A* in a broad population of patients with AIIG. We identified a Thai female (Pt-1) and a Saudi male (Pt-2) affected with AIIG. Both had hypoplastic enamel, gingival hyperplasia, and intrapulpal calcification. Pt-1 also had rapidly progressive embedding of unerupted teeth, early eruption of permanent teeth, and spontaneous dental infection. Uniquely, Pt-2 had all permanent teeth erupted which was uncommon in AIIG patients. Whole exome sequencing (WES) identified that Pt-1 was heterozygous for *FAM20A*, c.758A > G (p.Tyr253Cys), inherited from her father. The mutation on maternal allele was not detected by WES. Pt-2 possessed compound heterozygous mutations, c.1248dupG (p.Phe417Valfs*7); c.1081C > T (p.Arg361Cys) in *FAM20A*. Array comparative genomic hybridization (aCGH), cDNA sequencing, and whole genome sequencing successfully identified 7531 bp deletion on Pt-1's maternal allele. This was the largest *FAM20A* deletion ever found. A review of all 70 patients from 50 independent families with AIIG (including two families in this study) showed that the penetrance of hypoplastic enamel and gingival hyperplasia was complete. Unerupted permanent teeth were found in all 70 patients except Pt-2. Exons 1 and 11 were mutation-prone. Most mutations were frameshift. Certain variants showed founder effect. To conclude, this study reviews and expands phenotypic and genotypic spectra of AIIG. A large deletion missed by WES can be detected by WGS. Hypoplastic enamel, gingival hyperplasia, and unerupted permanent teeth prompt genetic testing of *FAM20A*. Screening of nephrocalcinosis, early removal of embedded teeth, and monitoring of dental infection are recommended.

Keywords Nephrocalcinosis · Gingival fibromatosis · Enamel hypoplasia · Biallelic · Autosomal recessive

Introduction

Amelogenesis imperfecta (AI) is a genetically and clinically heterogeneous group of disorders characterized by alterations in the structure and morphology of tooth enamel. Both primary and permanent dentitions are affected (Witkop 1988). The prevalence of AI ranges from 1:2000 to 18,000

(Sundell and Koch 1985; Backman and Holm 1986; Al-Salehi et al. 2009). It is classified as hypoplasia, hypocalcification, and hypomaturation based on clinical and radiographic characteristics (Aldred and Crawford 1995; Aldred et al. 2003; Crawford et al. 2007). However, AI can be associated with other orodental and/or systemic features such as enamel–renal syndrome (OMIM #204690) (Jaureguiberry et al. 2012), tricho–dento–osseous syndrome (OMIM #190320) (Crawford and Aldred 1990; Tim Wright et al. 1997), and jalili syndrome (OMIM #217080) (Michaelides et al. 2004). Biallelic loss-of-function mutations in *FAM20A* (family with sequence similarity 20, member A; OMIM *611,062) were first proposed to cause AI and gingival fibromatosis syndrome (O'Sullivan et al. 2011) and later with enamel–renal syndrome involving both AI and nephrocalcinosis (Jaureguiberry et al. 2012; Wang et al. 2013).

Communicated by Stefan Hohmann.

Electronic supplementary material The online version of this article (<https://doi.org/10.1007/s00438-020-01668-8>) contains supplementary material, which is available to authorized users.

✉ Thantrira Porntaveetus
thantrira.p@chula.ac.th

Extended author information available on the last page of the article

The syndromes are now considered as AI type IG (AI1G; OMIM #204690). To date, more than forty *FAM20A* mutations have been separately reported (Human Gene Mutation Database, HGMD®). Genetic heterogeneity regarding mutation types, majorly, small deletion, splicing, and nonsense; and phenotypic heterogeneity regarding enamel severity, oro-dental defects, and systemic involvement have been described. However, their genotypic and phenotypic spectra have never been summarized and analyzed. This study aimed to identify and summarize mutational and phenotypic spectra of AI1G to improve understanding of the disease and benefit genetic counseling for the families having AI1G and *FAM20A* mutations.

Here, two unrelated patients, a Thai female and a Saudi male, having AI1G were recruited for clinical and molecular studies. The mutations were first investigated by whole exome sequencing (WES). The variant missed by WES was delineated by array comparative genomic hybridisation (aCGH) and whole genome sequencing (WGS). Four novel mutations including the largest deletion in *FAM20A* were identified and validated by Sanger sequencing. A review and analysis of all patients previously reported with *FAM20A* mutations and those in this study were provided.

Materials and methods

Enrollment of human subjects

Two patients affected with hypoplastic AI were recruited in this study. One patient was from Thailand (Pt-1) and another one from Saudi Arabia (Pt-2). The study protocol was approved by the Human Ethical Review Board at the Faculty of Medicine, Chulalongkorn University, Thailand (IRB No.264/62). Clinical and radiographic examinations were performed. Blood and gingival samples were collected with the understanding and written consent of each participant according to the declaration of Helsinki.

Whole exome sequencing (WES) analysis

Genomic DNA was extracted from peripheral blood leukocytes using Gentra Puregene blood kit (Qiagen, Hilden, Germany) and sent to MacroGen, Inc. (Seoul, Korea) for WES (Porntaveetus et al. 2018). In brief, DNA libraries were prepared and enriched by SureSelect Human All Exon V5 (Agilent Technologies, Santa Clara, CA, USA). The enriched libraries were amplified and loaded into Illumina HiSeq 4000 sequencer. The raw sequencing data were mapped to the human reference genome hg19 using Burrows–Wheeler Aligner (BWA). Variant calling was

performed using Genome Analysis Toolkit (GATK) with HaplotypeCaller and annotated using SnpEff with annotation databases including a database of single nucleotide polymorphisms (dbSNP) 142, 1000Genome, ClinVar, and Exome Sequencing Project (ESP). The variants were filtered out if they were: (1) not in the genes related to amelogenesis imperfecta, (2) located in noncoding regions, (3) synonymous, and (4) found > 1% in the exome aggregation consortium (ExAC) database and our in-house database of 2,166 unrelated Thai exomes.

Array comparative genomic hybridization (aCGH)

Genomic DNA was extracted from peripheral blood leukocytes of the patient (Pt-1) and her mother using Gentra Puregene blood kit (Qiagen, Hilden, Germany). DNA labeling and hybridization were performed using the Agilent oligonucleotide array-based CGH according to the genomic DNA analysis protocol (V 7.3, 2014). Labeled test (Cy5) and reference (Cy3) DNA samples were paired and co-hybridized to the SurePrint G3 Human CGH Microarrays. The hybridized array was immediately scanned with an Agilent Microarray Scanner (Agilent Technologies, Inc.). The CGH data was extracted from the scanned images and translated into log₁₀ ratio of the normal DNA (Cy3) and test DNA (Cy5) signals using Agilent Feature Extraction software (v11.0.1.1). The raw data of log₁₀ ratio was transformed to log₂ ratio by the Agilent Genomic Workbench software. Aberrations were detected with the ADM-2 algorithm (threshold = 6.0) and aberration filtering options. Gains and losses were defined when the average linear log₂ ratio of 3 probes ≥ 0.25 or ≤ -0.25 , respectively.

cDNA sequencing

The RNA from Pt-1 was extracted from peripheral blood leukocytes using RNeasy Mini Kit (Qiagen, Hilden, Germany) and converted into cDNA using ImProm-II Reverse Transcription System (Promega, Wisconsin, USA). Polymerase chain reactions were carried out using two pairs of primers with cDNA as template (Supplementary Table 1).

Whole genome sequencing (WGS)

Genomic DNA was sent for WGS at BGI Inc (Beijing, China) using BGISEQ-500 Sequencer. The percentage of bases with Phred quality scores Q20 $\geq 90\%$, Q30 $\geq 80\%$, and average sequencing depth $\geq 40X$ were included. Sequence reads were aligned to the Human Reference Genome hg19/GRCh37 using BWA v.0.6.1 (Li and Durbin 2009). Variant calling was performed using GATK v4.0.1 (DePristo et al. 2011). To identify

the deletion breakpoint from short-read sequencing data (BAM file) in *FAM20A*, the variant detection algorithms including Genome Rearrangement OmniMapper (GROM) v1.0.1 (Smith et al. 2017), DELLY v0.7.8 (Rausch et al. 2012), Manta v1.3.2 (Chen et al. 2016), and our in-house software (Bolt) [manuscript in preparation] were employed. Based on the consensus deletion breakpoint from Manta, DELLY, and Bolt with the start and end positions of 66,530,405 and 66,537,936 on chromosome 17, the aligned reads covering these positions were then used for primer design.

Mutation validation

The variants identified by WES were validated by Sanger sequencing. The deletion was confirmed by Gap-PCR and Sanger sequencing (Supplementary Table 2). The PCR products were sent for sequencing at Macrogen, Inc. (Seoul, Korea). Sequence data were analyzed using Sequencher (V.5.0; Gene Codes Corporation, Ann Arbor, MI).

Alignment of *FAM20A* amino acid

Amino acid sequence of *Homo sapiens* *FAM20A* (NP_060035.2) and *FAM20C* (NP_064608.2) were aligned with *FAM20A* of other species including *Mus musculus* (NP_722477.1), *Bos taurus* (XP_002707814.2), *Gallus gallus* (XP_015135431.1), *Anolis carolinensis* (XP_003224754.1), *Xenopus tropicalis* (NP_001120441.1), *Danio rerio* (NP_001124252.1) and *Takifugu rubripes* (NP_001267023.1) by Clustal Omega multiple sequence alignment version 1.2.4.

Histology

Gingival tissue was obtained during gingivoplasty according to dental treatment plan. The gingiva sample was dehydrated through grade ethanol series, embedded in paraffin wax, sectioned, and stained with hematoxylin and eosin.

Reviews of genotype and phenotype of reported cases

Genotype and phenotype of reported cases with *FAM20A* mutation were accumulated by searching and reviewing literatures in PubMed and Google Scholar using “*FAM20A* mutation” as keyword. Phenotypic features of 68 individuals from 48 independent families with *FAM20A* mutations were found. Including our two patients from two independent families, the total number of patients with detailed phenotypes was 70 individuals from 50 independent families (Supplementary Table 3).

Results

Clinical characterization

The first proband (Pt-1) is a Thai girl. She first presented for dental treatment due to yellowish-brown teeth at 8.3 years of age. None of her family members had tooth discoloration. Her parents were non-consanguineous and healthy (Fig. 1a). Clinical and radiographic records showed that Pt-1 had severe enamel loss and early eruption of permanent teeth (Fig. 1b–e). Her chronological age was 8.3 years while dental age was 10.5 years (AlQahtani et al. 2010). At the age of 17 years, Pt-1 and her family were recruited for genetic studies. Oral examination of the proband revealed generalized hypoplastic enamel, gingival enlargement, high-arched palate, and incompetent lips. All of her teeth were restored with composite veneers. Radiographs exhibited skeletal class II malocclusion with normal maxilla and retrusive mandible, skeletal and dental anterior openbite, increased overjet, and prolonged retention of primary upper right canine. Multiple unerupted teeth including two upper canines, three second molars, and four third molars were noticed. The unerupted teeth showed hyperplastic dental follicles, thin enamel with reduced radiopacity, and concaved occlusal surface, suggesting pre-eruptive crown resorption. It was observed that the teeth were progressively embedded in the jaws with advanced age and showed accelerated crown resorption (Fig. 1f–h). Periapical radiographs showed narrow pulp cavities with heterotopic calcification (Fig. 1i). The upper right central incisor spontaneously developed abscess and required endodontic treatment (Fig. 1j). After the impacted teeth were surgically removed at the age of 18 years, the patient developed hypoesthesia at her lower lip and left cheek and oro-antral communication for few months. Gingival biopsy revealed a thick dense layer of fibrocollagenous connective tissue and parakeratinizing stratified squamous epithelium with matured epithelial cells, indicating gingival hyperplasia (Fig. 1k). The renal and chest radiographs did not show abnormal calcifications (Fig. 1l, m). Renal function test was within the normal range.

The second proband (Pt-2), 28 years of age, was from Saudi Arabia. He presented with discolored teeth and dental hypersensitivity. His younger sister and brother also had brown teeth. His parents were consanguineous and had healthy teeth (Fig. 2a). Oral examination of Pt-2 revealed the eruption of all 32 permanent teeth, yellowish-brown and pitted enamel, tooth attrition and erosion, multiple cavities, and anterior openbite. His gingiva was enlarged, pigmented, and inflamed (Fig. 2b, c). Dental radiographs revealed loss of enamel with reduced radiodensity,

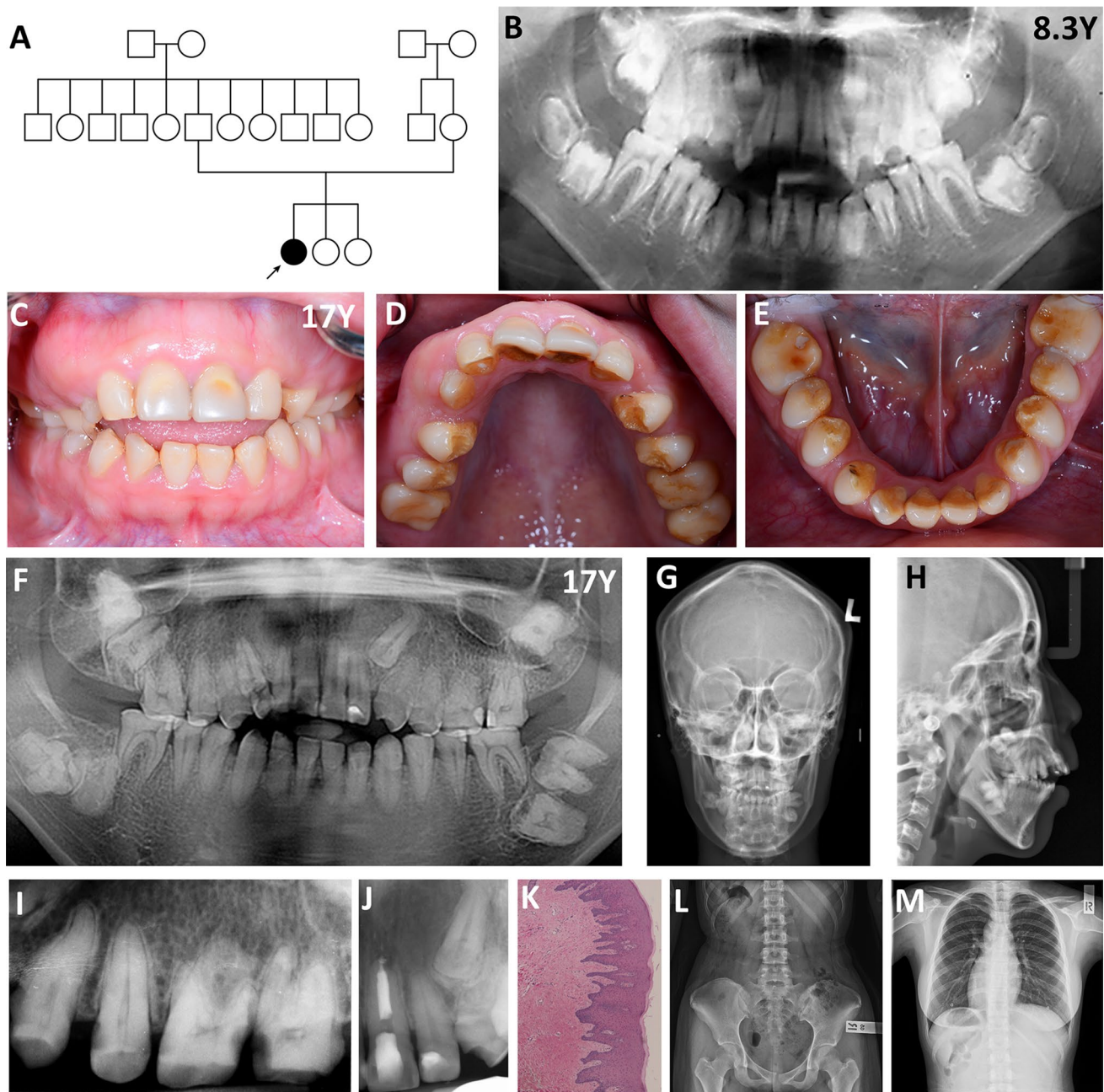


Fig. 1 Pedigree, photographs, and radiographs Pt-1. **a** Pedigree of the family. Proband is indicated with black arrow **b** Panoramic radiograph at age 8.3 years showed hypoplastic enamel and early eruption of permanent teeth **c–e** Oral photographs at age 17 years revealed generalized hypoplastic enamel, gingival enlargement, minimal interproximal contacts, and high-arched palate. The teeth were restored with direct resin composite **f–h** Radiographs at age 17 years exhibited skeletal class II malocclusion, anterior openbite, prolong retention of primary maxillary right canine, and multiple unerupted teeth includ-

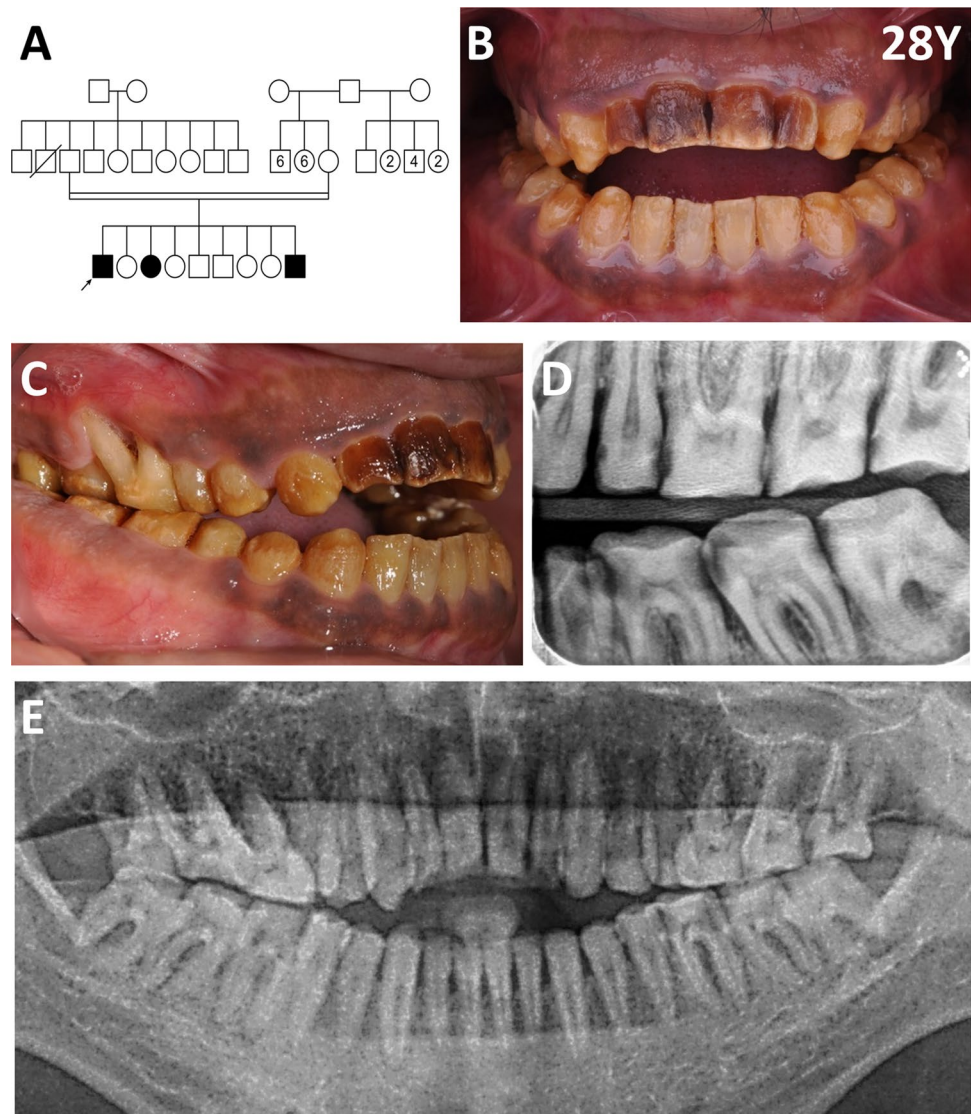
ing two upper canines, three second molars, and four third molars. The upper third molars were superimposed on the maxillary sinus whereas the lower second and third molars were adjacent to the inferior alveolar canal and lower border of the mandible. **i** Heterotopic calcification was found in the dental pulps. **j** The upper right central incisor had endodontic treatment. **k** The histology revealed gingival hyperplasia showing a thick dense layer of fibrocollagenous connective tissue and parakeratinizing stratified squamous epithelium. **l, m** Renal and chest radiographs were unremarkable

multiple proximal cavities, and alveolar bone loss with furcation involvement in the posterior teeth (Fig. 2d, e). His upper right molars showed large periapical lesion indicating dental infection.

WES analysis

Genetic investigations using singleton WES identified that Pt-1 possessed a novel heterozygous missense mutation,

Fig. 2 Pedigree, photographs, and radiographs of Pt-2. **a** Pedigree of the family. Proband is indicated with black arrow. **b, c** Frontal and lateral views of oral cavity revealed brown, pitted, and hypoplastic enamel, anterior openbite, and gingival hyperpigmentation and inflammation. **d, e** Bitewing and panoramic radiographs exhibited loss of enamel, dental cavities, alveolar bone loss, furcation involvement, and periapical radiolucency



c.758A > G (p.Tyr253Cys), in exon 5 of *FAM20A* which was inherited from her father. This variant was predicted to be deleterious (SIFT: 0.0), damaging (PolyPhen: 1.0), and possibly pathogenic (M-CAP: 0.119). The Tyr253 was conserved among a broad range of species (Supplementary Fig. 1). The mutation on the maternal allele was not detected by WES.

For Pt-2, WES identified the novel compound heterozygous mutations, c.1248dupG (p.Phe417Valfs*7) in exon 9 and c.1081C > T (p.Arg361Cys) in exon 7 of *FAM20A*. The p.Arg361Cys was predicted to be deleterious (SIFT: 0.0), damaging (PolyPhen: 1.0), and possibly pathogenic (M-CAP: 0.316). The Arg361 was conserved among several species (Supplementary Fig. 1).

Identification of large deletion on the maternal allele of Pt-1

Given the recessive inheritance pattern of *FAM20A* mutations, aCGH and cDNA sequencing were employed to determine whether the second mutation involved large deletions/insertions and deep intronic mutations, respectively. aCGH suggested a deletion of exons 8–11 in *FAM20A*. cDNA sequencing with a pair of primers capturing exons 1 and 6 revealed the heterozygosity of c.758A > G located in exon 5, while that with primers capturing exons 4 and 11 showed only the G at position c.758. This loss of heterozygosity is consistent with the deletion involving exon 11 of the maternal allele. WGS was then performed. It was able to specify the 7531 bp deletion starting at 90 bp downstream of exon 7 and ending at

852 bp downstream of exon 11 in *FAM20A*. This mutation was novel and the largest deletion reported in *FAM20A*. The deletion was confirmed by gap-PCR and Sanger sequencing (Supplementary Figs. 2 and 3).

Phenotypes of patients with *FAM20A* mutations

In addition to two patients in this study, we reviewed 68 patients from 48 families previously reported with *FAM20A* mutations. The total number was 70 affected patients from 50 families. The consistent phenotypic features of all patients were generalized hypoplastic enamel and gingival hyperplasia (100%, 70/70). Of 41 patients with radiographic data, 40 except Pt-2 had unerupted/impacted permanent teeth (97.6%). The unerupted teeth were mostly in the posterior segment. They showed pre-eruptive crown resorption and pericoronal radiolucency. Other frequently found oral anomalies were intrapulpal calcification, prolonged retention of deciduous teeth, malocclusion, and periodontal defects. Inconsistently, renal calcification and deviated blood and urine biochemistry were reported. The phenotypes and genotypes of 50 families with *FAM20A* mutations are demonstrated in Supplementary Table 3.

Genotypes of patients with *FAM20A* mutations

Of 50 affected families, a total of 100 mutant alleles were analyzed. Overall, the mutations were most commonly located in exon 11 (24%), followed by exon 1 (18%), and exon 6 (9%) (Fig. 3a, b, Supplementary Table 4). The common types of variants were frameshift (58%), nonsense (16%), missense (12%), and splice site (11%). Inframe deletion, large deletion, and large duplication were found at one percent each (Fig. 3c, d). Of 100 *FAM20A* mutations, c.34_35delCT (p.Leu12Alafs*67) in exon 1 was the most common (11%), followed by c.1447delG (p.Glu483Lysfs*24) in exon 11 (10%), and c.406C>T (p.Arg136*) in exon 2 ($n = 7\%$), respectively. Certain variants were found in more than one family with the same ethnicity. Those included c.1447delG in Brazilian, c.34_35delCT in Turkish, and c.349_367delCTGGCCAGCCAGGAGGCGC in Thai populations (Supplementary Table 5).

Discussion

Since homozygous nonsense mutations in *FAM20A* were proposed for the first time to cause amelogenesis imperfecta and gingival hyperplasia syndrome (AIIG) (O'Sullivan et al. 2011), 50 families with one hundred mutations in *FAM20A* have been identified. Despite many cases, its genotype and

phenotype spectra remain to be analyzed. Here, we reviewed all patients previously reported with *FAM20A* mutations and reported the other two unrelated patients having AIIG and four novel *FAM20A* mutations.

Generalized hypoplastic enamel and gingival hyperplasia were completely penetrant in patients with *FAM20A* mutations (Cho et al. 2012; Jaureguiberry et al. 2012; Koruyucu et al. 2018). The teeth with enamel hypoplasia were rapidly deteriorated and could cause dental arch spacing, malocclusion, and decreased vertical dimension. Other findings frequently observed were unerupted permanent teeth, prolonged retention of deciduous teeth, intrapulpal calcification, malocclusion, and periodontal defects. Impacted teeth often showed root dilacerations. These clinical and radiographic findings could prompt the dental professionals to speculate mutations in *FAM20A*.

Phenotypically, the unique characteristics of Pt-1 were early eruption of permanent teeth, rapidly progressive embedding of unerupted teeth, and spontaneous dental infection. The cause of tooth infection was likely to be the ectopic pulp stones and weak enamel. We noticed that the impacted teeth were located deeper in the jaw with advanced age. Considering the progressive deterioration of unerupted teeth, they could cause complications after surgery. Thus, patients diagnosed with *FAM20A* mutations should receive early intervention to remove the embedded teeth. In addition, the affected teeth with intrapulpal calcification should be radiographically monitored to avoid extensive dental infection. To the best of our knowledge, Pt-2 was the only AIIG patient who had all his 32 permanent teeth erupted. This shows for the first time that the unerupted permanent teeth feature is not fully penetrant in AIIG.

Nephrocalcinosis in AIIG might not be found at young ages (de la Dure-Molla et al. 2014). Renal calcification was not detected in Pt-1 at the age of 17 years and sign of kidney problem was not noticed in Pt-2 at the age of 28 years. To date, a solid correlation between nephrocalcinosis and *FAM20A* mutation cannot be drawn. It is also unpredictable when renal stones are of clinical significance. We therefore recommend that renal condition in the patients with AIIG should be regularly monitored.

WES has been increasingly utilized for diagnosis of rare diseases due to its superior diagnostic yield over traditional genetic tests and declining cost of sequencing (Sawyer et al. 2016; Vissers et al. 2017; Dillon et al. 2018). Using WES, we detected biallelic *FAM20A* mutations in Pt-2 and monoallelic mutation in Pt-1. Considering the clinical features of Pt-1 which was consistent AIIG and biallelic nature of *FAM20A* mutations, the second variant on another allele was expected in Pt-1. aCGH was next selected to determine a large deletion or insertion in *FAM20A* which might be missed by WES. In addition, cDNA sequencing was employed to explore point mutation in deep intronic

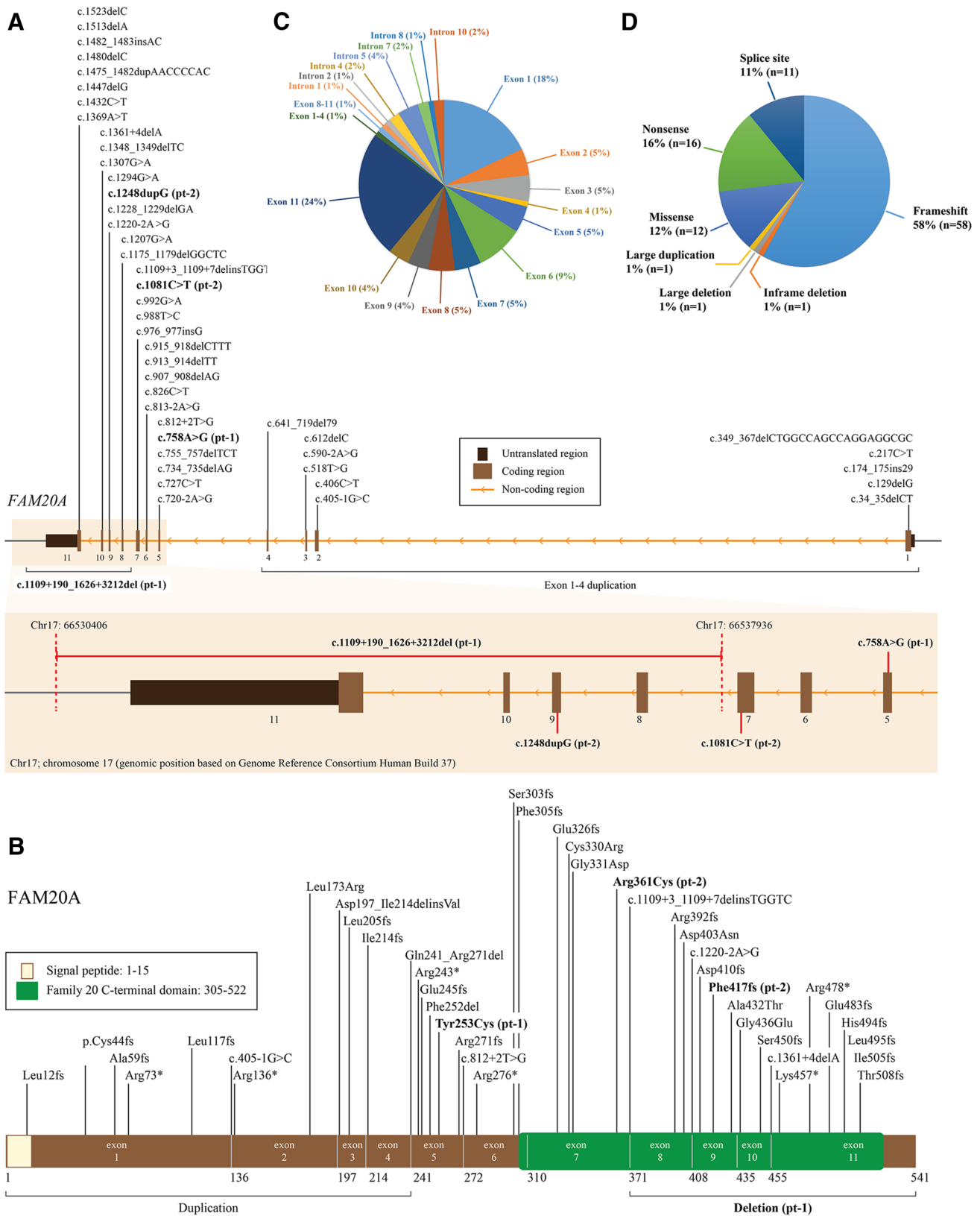


Fig. 3 Summary of *FAM20A* mutations previously reported and identified in this study. **a**, **b** Schematic diagram of the *FAM20A* gene and protein demonstrated all identified mutations. **c** A pie chart illustrated

the location of mutations according to exon. **d** A pie chart categorized the type of mutations

region. Using aCGH and cDNA sequencing, a large deletion involving exons 8–11 of *FAM20A* was detected. Then, the deletion breakpoints were spotted by WGS. It revealed the 7531 bp deletion spanning exons 8–11 of *FAM20A* on the Pt-1's maternal allele. The mutations were all validated by Sanger sequencing.

With combined techniques, all four mutations in the two patients were detected. Pt-1 was compound heterozygous for the largest deletion spanning exons 8–11 and the missense mutation (c.758A > G, p.Tyr253Cys). Pt-2 was compound heterozygous for the frameshift mutation (c.1248dupG, p.Phe417Valfs*7) and the missense mutation (c.1081C > T, p.Arg361Cys) in *FAM20A*.

Our comprehensive review of all cases reported with *FAM20A* mutations revealed that frameshift mutation accounted for 58%, followed by nonsense, missense, and splice site. The mutations were frequently located in the last exon (exon 11, 24%) and the first exon (18%). The c.34_35delCT (p.Leu12Alafs*67) in exon 1, c.1447delG (p.Glu483Lysfs*24) in exon 11 ($n = 10/100$), and c.406C > T (p.Arg136*) in exon 2 were the top three common variants. The c.1447delG (p.Glu483Lysfs*24) was only present in Brazilians and c.349_367delCTGGCCAGCCAGGAGGCG C (p.Leu117Cysfs*22) in Thais. These imply the founder effect of these variants in the Brazilian and Thai populations, respectively.

To conclude, this study identifies four novel *FAM20A* mutations including the largest deletion ever reported and demonstrates genetic approaches to identify large gene deletions. A patient in this study is the first *FAM20A* patient who has all permanent teeth erupted. These expand the genotypic and phenotypic spectra of *FAM20A* mutation. Due to the progressive nature of nephrocalcinosis and embedded teeth, the patients should be regularly monitored by medical and dental professionals.

Acknowledgements We thank Trakarn Sookthonglarng, Yuttupong Kunchanapruet, Lawan Boonprakong, and Anucharte Srijunbarl for laboratory assistance.

Funding This study was supported by the 90th anniversary of Chulalongkorn University, Ratchadapisek Somphot Endowment Fund, Medical Genomics Cluster, Faculty of Dentistry (DRF63004), Chulalongkorn academic advancement into its second century project, and Thailand research fund (RSA6280001, DPG6180001).

Data availability The datasets generated during and/or analyzed during the current study are available from the corresponding author on reasonable request.

Compliance with ethical standards

Conflict of interest The authors declare that they have no competing interests.

Ethical approval All procedures performed in studies involving human participants were in accordance with the ethical standards of the institutional and/or national research committee and with the 1964 Helsinki Declaration and its later amendments or comparable ethical standards. The study was approved by the Human Ethical Review Board at the Faculty of Medicine, Chulalongkorn University, Thailand (IRB No.264/62).

Informed consent Written informed consent was obtained from all participants or their guardians.

References

- Al-Salehi SK, Dooley K, Harris IR (2009) Restoring function and aesthetics in a patient previously treated for amelogenesis imperfecta. *Eur J Prosthodont Restor Dent* 17:170–176
- Aldred M, Crawford P (1995) Amelogenesis imperfecta—towards a new classification. *Oral Dis* 1:2–5
- Aldred M, Crawford P, Savarirayan R (2003) Amelogenesis imperfecta—a classification and catalogue for the 21st century. *Oral Dis* 9:19–23
- AlQahtani SJ, Hector MP, Liversidge HM (2010) Brief communication: The London atlas of human tooth development and eruption. *Am J Phys Anthropol* 142:481–490
- Backman B, Holm AK (1986) Amelogenesis imperfecta: prevalence and incidence in a northern Swedish county. *Commun Dent Oral Epidemiol* 14:43–47
- Chen X, Schulz-Trieglaff O, Shaw R, Barnes B, Schlesinger F, Kallberg M, Cox AJ, Kruglyak S, Saunders CT (2016) Manta: rapid detection of structural variants and indels for germline and cancer sequencing applications. *Bioinformatics* 32:1220–1222
- Cho SH, Seymen F, Lee K-E, Lee S-K, Kweon Y-S, Kim KJ, Jung S-E, Song SJ, Yildirim M, Bayram M, Tuna EB, Gencay K, Kim J-W (2012) Novel *FAM20A* mutations in hypoplastic amelogenesis imperfecta. *Hum Mutat* 33:91–94
- Crawford P, Aldred M, Bloch-Zupan A (2007) Amelogenesis imperfecta. *Orphanet J Rare Dis* 2:17
- Crawford PJM, Aldred MJ (1990) Amelogenesis imperfecta with taurodontism and the tricho-dento-osseous syndrome: separate conditions or a spectrum of disease? *Clin Genet* 38:44–50
- de la Dure-Molla M, Quentric M, Yamaguti PM, Acevedo AC, Mighell AJ, Vikkula M, Huckert M, Berald A, Bloch-Zupan A (2014) Pathognomonic oral profile of Enamel Renal Syndrome (ERS) caused by recessive *FAM20A* mutations. *Orphanet J Rare Dis* 9:84
- DePristo MA, Banks E, Poplin R, Garimella KV, Maguire JR, Hartl C, Philippakis AA, del Angel G, Rivas MA, Hanna M, McKenna A, Fennell TJ, Kernytsky AM, Sivachenko AY, Cibulskis K, Gabriel SB, Altshuler D, Daly MJ (2011) A framework for variation discovery and genotyping using next-generation DNA sequencing data. *Nat Genet* 43:491–498
- Dillon OJ, Lunke S, Stark Z, Yeung A, Thorne N, Gaff C, White SM, Tan TY (2018) Exome sequencing has higher diagnostic yield compared to simulated disease-specific panels in children with suspected monogenic disorders. *Eur J Hum Genet* 26:644–651
- Jaureguiberry G, De la Dure-Molla M, Parry D, Quentric M, Himmerkus N, Koike T, Poulter J, Klootwijk E, Robinette SL, Howie AJ, Patel V, Figueres ML, Stanescu HC, Issler N, Nicholson JK, Bockenbauer D, Laing C, Walsh SB, McCredie DA, Povey S, Asselin A, Picard A, Coulomb A, Medlar AJ, Bailleul-Forestier I, Verloes A, Le Caignec C, Roussey G, Guiol J, Isidor B, Logan C, Shore R, Johnson C, Inglehearn C, Al-Bahlani S, Schmittbuhl M, Clauss F, Huckert M, Laugel V, Ginglinger E, Pajarola S, Sparta

- G, Bartholdi D, Rauch A, Addor MC, Yamaguti PM, Safatle HP, Acevedo AC, Martelli-Junior H, dos Santos Netos PE, Coletta RD, Gruessel S, Sandmann C, Ruehmann D, Langman CB, Scheinman SJ, Ozdemir-Ozenen D, Hart TC, Hart PS, Neugebauer U, Schlatter E, Houillier P, Gahl WA, Vikkula M, Bloch-Zupan A, Bleich M, Kitagawa H, Unwin RJ, Mighell A, Berdal A, Kleta R (2012) Nephrocalcinosis (enamel renal syndrome) caused by autosomal recessive FAM20A mutations. *Nephron Physiol* 122:1–6
- Koruyucu M, Seymen F, Gencay G, Gencay K, Tuna EB, Shin TJ, Hyun HK, Kim YJ, Kim JW (2018) Nephrocalcinosis in Amelogenesis Imperfecta Caused by the FAM20A Mutation. *Nephron* 139:189–196
- Li H, Durbin R (2009) Fast and accurate short read alignment with Burrows–Wheeler transform. *Bioinformatics* 25:1754–1760
- Michaelides M, Bloch-Zupan A, Holder G, Hunt D, Moore A (2004) An autosomal recessive cone-rod dystrophy associated with amelogenesis imperfecta. *J Med Genet* 41:468–473
- O’Sullivan J, Bitu CC, Daly SB, Urquhart JE, Barron MJ, Bhaskar SS, Martelli-Junior H, dos Santos Neto PE, Mansilla MA, Murray JC, Coletta RD, Black GC, Dixon MJ (2011) Whole-Exome sequencing identifies FAM20A mutations as a cause of amelogenesis imperfecta and gingival hyperplasia syndrome. *Am J Hum Genet* 88:616–620
- Porntaveetus T, Abid MF, Theerapanon T, Srichomthong C, Ohazama A, Kawasaki K, Kawasaki M, Suphapeetiporn K, Sharpe PT, Shotelersuk V (2018) Expanding the oro-dental and mutational spectra of kabuki syndrome and expression of KMT2D and KDM6A in human tooth germs. *Int J Biol Sci* 14:381–389
- Rausch T, Zichner T, Schlattl A, Stutz AM, Benes V, Korbel JO (2012) DELLY: structural variant discovery by integrated paired-end and split-read analysis. *Bioinformatics* 28:i333–i339
- Sawyer SL, Hartley T, Dymont DA, Beaulieu CL, Schwartzentruber J, Smith A, Bedford HM, Bernard G, Bernier FP, Brais B, Bulman DE, Warman Chardon J, Chitayat D, Deladoëy J, Fernandez BA, Frosk P, Geraghty MT, Gerull B, Gibson W, Gow RM, Graham GE, Green JS, Heon E, Horvath G, Innes AM, Jabado N, Kim RH, Koeneke RK, Khan A, Lehmann OJ, Mendoza-Londono R, Michaud JL, Nikkel SM, Penney LS, Polychronakos C, Richer J, Rouleau GA, Samuels ME, Siu VM, Suchowersky O, Tarnopolsky MA, Yoon G, Zahir FR, Consortium FC, C Care4Rare Canada, Majewski J, Boycott KM (2016) Utility of whole-exome sequencing for those near the end of the diagnostic odyssey: time to address gaps in care. *Clin Genet* 89(275):284
- Smith SD, Kawash JK, Grigoriev A (2017) Lightning-fast genome variant detection with GROM. *Gigascience* 6:1–7
- Sundell S, Koch G (1985) Hereditary amelogenesis imperfecta. I. Epidemiology and clinical classification in a Swedish child population. *Swed Dent J* 9:157–169
- Tim Wright J, Kula K, Hall K, Simmons JH, Hart TC (1997) Analysis of the tricho-dento-osseous syndrome genotype and phenotype. *Am J Med Genet* 72:197–204
- Visser LELM, van Nimwegen KJM, Schieving JH, Kamsteeg E-J, Kleefstra T, Yntema HG, Pfundt R, van der Wilt GJ, Krabbenborg L, Brunner HG, van der Burg S, Grutters J, Veltman JA, Willemssen MAAP (2017) A clinical utility study of exome sequencing versus conventional genetic testing in pediatric neurology. *Genet Med* 19:1055
- Wang SK, Aref P, Hu Y, Milkovich RN, Simmer JP, El-Khateeb M, Daggag H, Baqain ZH, Hu JC (2013) FAM20A mutations can cause enamel-renal syndrome (ERS). *PLoS Genet* 9:e1003302
- Witkop CJ (1988) Amelogenesis imperfecta, dentinogenesis imperfecta and dentin dysplasia revisited: problems in classification. *J Oral Pathol* 17:547–553

Publisher’s Note Springer Nature remains neutral with regard to jurisdictional claims in published maps and institutional affiliations.

Affiliations

Issree Nitayavardhana¹ · Thanakorn Theerapanon^{2,3} · Chalurmporn Srichomthong^{4,5} · Sakkayaphab Piwluang⁶ · Duangdao Wichadaku^{7,8,9} · Thanrira Porntaveetus^{1,2}  · Vorasuk Shotelersuk^{4,5}

¹ Geriatric Dentistry and Special Patients Care International Program, Faculty of Dentistry, Chulalongkorn University, Bangkok 10330, Thailand

² Genomics and Precision Dentistry Research Unit, Department of Physiology, Faculty of Dentistry, Chulalongkorn University, Bangkok 10330, Thailand

³ Center of Excellence for Regenerative Dentistry, Faculty of Dentistry, Chulalongkorn University, Bangkok 10330, Thailand

⁴ Center of Excellence for Medical Genomics, Medical Genomics Cluster, Department of Pediatrics, Faculty of Medicine, Chulalongkorn University, Bangkok 10330, Thailand

⁵ Excellence Center for Genomics and Precision Medicine, King Chulalongkorn Memorial Hospital, The Thai Red Cross Society, Bangkok 10330, Thailand

⁶ Department of Computer Engineering, Master of Science in Software Engineering Program, Faculty of Engineering, Chulalongkorn University, Bangkok 10330, Thailand

⁷ Chulalongkorn Big Data Analytics and IoT Center (CUBIC), Department of Computer Engineering, Faculty of Engineering, Chulalongkorn University, Bangkok 10330, Thailand

⁸ Center of Excellence in Systems Biology, Faculty of Medicine, Chulalongkorn University, Bangkok 10330, Thailand

⁹ Research Group on Applied Computer Engineering Technology for Medicine and Healthcare, Faculty of Engineering, Chulalongkorn University, Bangkok 10330, Thailand